UNIVERSITY OF LOUISVILLE®
SCHOOL OF MEDICINE

Understanding the Role of Hydralazine as an Epigenetic Cancer Therapy in Relation to *N*-Acetyltransferase Acetylator Phenotype

Cecily E. Allen, Mark A. Doll, David W. Hein
Department of Pharmacology and Toxicology
University of Louisville School of Medicine

Introduction

- *N*- Acetyltransferases (NATs) are acetylating enzymes. NAT1 and NAT2 are isozymes. NAT2 is distributed in the intestines and liver, and is involved in phase II drug metabolism of arylamines and arylhydrazines. NAT2 has single nucleotide polymorphisms (SNPs) that result in different acetylation rates that impact drug metabolism including: rapid, intermediate, and slow acetylating phenotypes.
- Hydralazine is a drug used in resistant hypertension and is subject to acetylation by NAT2. Earliest studies evidenced a tri-modal distribution of acetylating phenotypes (rapid, intermediate, and slow), while more recent, smaller studies demonstrated bimodal (rapid and slow) acetylating phenotypes.
- Recent studies demonstrated that hydralazine also acts as an epigenetic modulator within neoplastic cells, aiding in the re-expression of tumor suppressor genes, increasing apoptosis, and inhibiting cell growth. In addition, hydralazine decreases resistance to certain cancer chemotherapies.
- Clinical trials using hydralazine are dosing based on NAT2 genotype, but the studies do not show evidence to support the quantifiable differences in hydralazine efficacy based on the current dosing regimen that is only dosing for differences in rapid and slow acetylators.

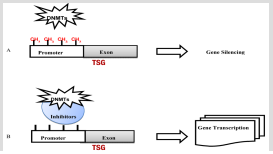

***Diagram 1*. A**- cancer phenotype with hyper-methylated promotor of tumor suppressor genes. **B**- impact of hydralazine, a DNMTi, allowing for re-expression of tumor suppressor genes and changing the cancer phenotype[1] .

Hypothesis

If hydralazine is shown to be metabolized by NAT, and NAT2 is the primary acetylating enzyme, then quantifiable differences in the amount of hydralazine available to modulate cellular epigenetics should be measured in human hepatocytes to understand the drug's metabolism based on NAT2 acetylating phenotype (rapid, intermediate, or slow). This understanding will allow patients to be dosed based on the quantitative differences in hydralazine availability according to their NAT2 genotype, specific SNPs, and acetylating index so that the maximal therapeutic benefit can be achieved for rapid, intermediate, and slow acetylators.

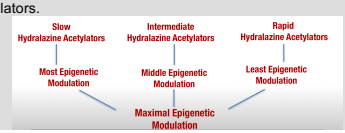

Methods

- **Determination of NAT1 vs NAT2 hydralazine enzyme kinetics**
  - Yeast lysates of human recombinant NAT1 and NAT2 were used in independent reactions with hydralazine to determine the Km and Vmax. Quantification of the amount of product produced during reactions was determined using HPLC. These reactions established the enzyme kinetics for each isozyme.
- **In vitro determination of acetylation rates due to NAT2 genotype**
  - Cryopreserved human hepatocyte lysates of rapid, intermediate, and slow genotypes were used in reactions with hydralazine and acetyl coenzyme A. The same experiment was run with slow NAT2 SNPs to determine the presence of an acetylating index. Quantification of the amount of product produced during reactions was determined using HPLC. These reactions established if the different NAT2 genotypes manifested in phenotypic variation of acetylation of hydralazine with human hepatocyte lysates.
- **In situ determination of acetylation rates due to NAT2 genotype**
  - Cryopreserved human hepatocytes of all three NAT2 genotypes were plated for 48 hours, washed with PBS and then cultured with PBS + dextrose and hydralazine for 12 hours, with samples taken every 4 hours. Samples of the media were run on HPLC in order to quantify the amount of acetylated hydralazine produced for each genotype within a human hepatocyte.

Results

- **Determination of NAT1 vs NAT2 hydralazine enzyme kinetics**
  - NAT2 has a lower apparent Km, signifying increased affinity for hydralazine when compared to NAT1. (Figure 1.A). Also, NAT2 has a higher Vmax, resulting in increased production of acetylated hydralazine, when compared with NAT1. (Figure 1.B). Thus, NAT2 has a higher substrate clearance of hydralazine (Figure 1.C).
- **In vitro determination of acetylation rates due to NAT2 genotype**
  - At multiple concentrations, the different NAT2 genotypes resulted in quantifiable differences in acetylation rates of hydralazine with rapid acetylators producing the most acetylated product, intermediate acetylators producing intermediate levels, and slow acetylators yielding the least acetylated hydralazine in the same period of time. (Figure 2. A, B, C). This trend was statistically significant and evidenced at different concentrations including:1000 μM hydralazine p< 0.005; 100 μM hydralazine p<0.001; 10 μM hydralazine p<0.001 .
  - Phenotypic heterogeneity in the amount of acetylated hydralazine was observed in the different slow acetylating NAT2 SNPs p<0.001. (Figure 2.D).
- **In situ determination of acetylation rates due to NAT2 genotype**
  - There was a concentration dependent response in the amount of acetylated hydralazine produced. This trend evidences increased acetylated product at higher doses of hydralazine. (Figure 3.A). Additionally, there was a time dependent increase in the amount of acetylated hydralazine produced. This trend was evidenced at multiple hydralazine concentrations. (Figure 3.B).
  - Differences in rapid, intermediate, and slow acetylators resulted in different amounts of acetylated hydralazine at multiple concentrations in cultured cryopreserved hepatocytes.
  - There was a genotype and concentration-dependent increase in the amount of acetylated hydralazine produced. Rapid, intermediate, and slow acetylators producing the most, intermediate, and the least acetylated hydralazine respectively at 10 μM hydralazine (p=0.002) (Figure 4.A) and 100 μM hydralazine (p=0.0015) (Figure 4.B).

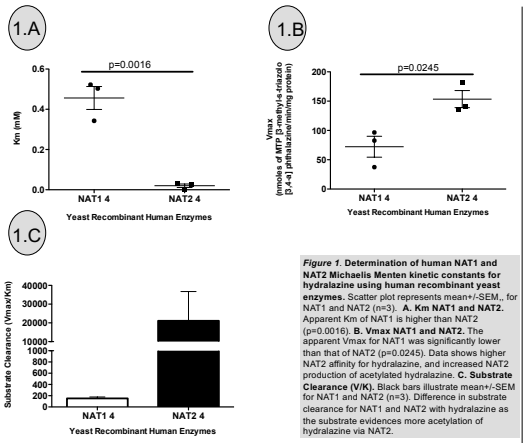

***Figure 1*. Determination of human NAT1 and NAT2 Michaelis Menten kinetic constants for hydralazine using human recombinant yeast enzymes.** Scatter plot represents mean+/-SEM,. for NAT1 and NAT2 (n=3). **A. Km NAT1 and NAT2.** Apparent Km of NAT1 is higher than NAT2 (p=0.0016). **B. Vmax NAT1 and NAT2.** The apparent Vmax for NAT1 was significantly lower than that of NAT2 (p=0.0245). Data shows higher NAT2 affinity for hydralazine, and increased NAT2 production of acetylated hydralazine. **C. Substrate Clearance (V/K).** Black bars illustrate mean+/-SEM for NAT1 and NAT2 (n=3). Difference in substrate clearance for NAT1 and NAT2 with hydralazine as the substrate evidences more acetylation of hydralazine via NAT2.

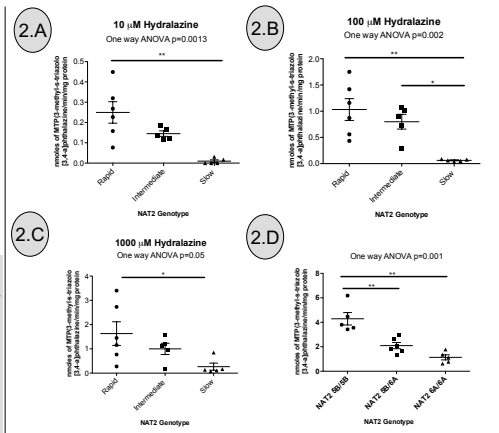

***Figure 2*. In-Vitro *N*-Acetylation of hydralazine by human hepatocyte lysates.** Scatter plots represent mean+/-SEM illustrates the results from in vitro hepatocyte lysate reactions. Genotypes of rapid (N=6), intermediate (N=5), and slow (N=5). Data evidences phenotypic variation with acetylation of hydralazine at varying concentrations. **A. 10 μM hydralazine.** The amount of acetylated product differed significantly with respect to NAT2 genotype (p=0.0013). **B. 100 μM hydralazine.** Data evidences phenotypic variation with acetylation of hydralazine at varying concentrations. The amount of acetylated product differed significantly with respect to NAT2 genotype (p=0.002). **C. 1000 μM hydralazine.** The amount of acetylated product differed significantly with respect to NAT2 genotype (p=0.05). Data supports a phenotypic variation in the amount of acetylated product yielded, with rapids producing the most, intermediate producing middle, and slow acetylators the least acetylated hydralazine. **D. Slow SNPs genotypic variation.** Slow acetylating genotypes were NAT2 *5B/*5B (n=5), NAT2 *5B/*6A (n=6), and NAT2 *6A/*6A (n=5). Data evidences a phenotypic variation among the slow acetylating NAT2 genotypes (p=0.001)

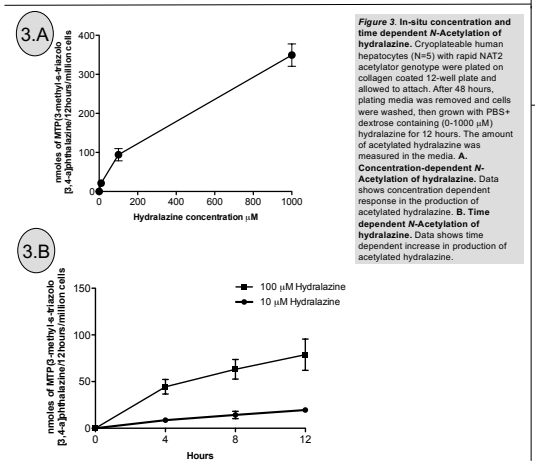

***Figure 3*. In-situ concentration and time dependent *N*-Acetylation of hydralazine.** Cryopleateable human hepatocytes (N=5) with rapid NAT2 acetylator genotype were plated on collagen coated 12-well plate and allowed to attach. After 48 hours, plating media was removed and cells were washed, then grown with PBS+ dextrose containing (0-1000 μM) hydralazine for 12 hours. The amount of acetylated hydralazine was measured in the media. **A. Concentration-dependent *N*-Acetylation of hydralazine.** Data shows concentration dependent response in the production of acetylated hydralazine. **B. Time dependent *N*-Acetylation of hydralazine.** Data shows time dependent increase in production of acetylated hydralazine.

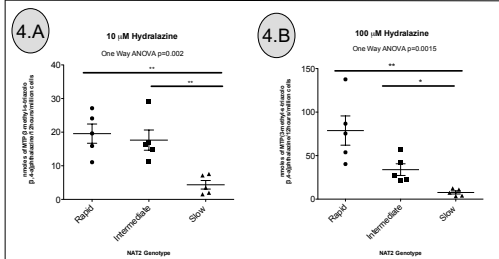

***Figure 4*. In-situ genotype dependent *N*-Acetylation of hydralazine.** Cryoplateable human hepatocytes were plated on collagen coated 12-well plate and allowed to attach. After 48 h plating media was removed and cells were washed, then grown with PBS + dextrose containing 10 μM or 100 μM Hydralazine for 12 h. the amount of acetylated hydralazine was measured in the media. Scatter plots illustrate mean +/-SEM activities in rapid (n=5), intermediate (n=5) and slow (n=5) acetylators. **A. 10 μM Hydralazine. B. 100 μM hydralazine.** One way ANOVA demonstrates statistical significance at both 10 and 100 μM concentrations of hydralazine for in situ N-acetylation of hydralazine with p-value of p=0.002 and p=.0015 respectively.

Conclusions

- **Determination of NAT1 vs NAT2 hydralazine enzyme kinetics**
  - With respect to enzyme kinetics, NAT2 is the primary NAT responsible for the acetylation of hydralazine at therapeutic concentrations based on the lower Km, signifying increased affinity. The Vmax and substrate clearance were also higher for NAT2.
- **In vitro determination of acetylation rates due to NAT2 genotype**
  - With respect to in vitro acetylation studies, acetylation of hydralazine is NAT2 genotype-dependent. With more acetylated product being produced in rapids, intermediates having intermediate levels, and slow acetylators producing the least. This supports a tri-modal hydralazine acetylation model.
  - Slow acetylating SNPs illustrate genetic heterogeneity supporting the presence of a hydralazine acetylating index that varies within the slow NAT2 phenotype, based on the specific SNPs present in the genotype.
- **In Situ determination of acetylation rates due to NAT2 genotype**
  - There is a time and concentration dependent response in hydralazine acetylation rates, with more product being yielded with more culture time and increased dosing concentrations of hydralazine.
  - With respect to in situ acetylation studies, acetylation of hydralazine is NAT2 genotype-dependent. With more acetylated product being produced in rapid genotypes, intermediated producing moderate and the least in slow acetylating genotypes. This further confirms a tri-modal acetylating model.

Clinical Significance/ Future Direction

- **Clinical significance**
  - These results evidence two layers of complexity when finding the appropriate dosing regimen for hydralazine so that maximal epigenetic modulation and efficacy for all NAT2 acetylating genotypes: tri-modal model of acetylation and phenotypic variation for a given slow acetylator phenotype based on SNPs (ie. slow acetylator phenotype heterogeneity).
  - Future direction should include quantifying the difference in epigenetic modulation based on NAT2 genotype and specific SNPs for a data driven dosing regimen with equivalent therapeutic efficacy based on a tri-modal hydralazine acetylating index.

Acknowledgements and References

1. Majed S. Alokail and Amal M. Alenad (2015). DNA Methylation, A Concise Review of Molecular Pathology of Breast Cancer, Prof. Mehmet Gunduz (Ed.), InTech, DOI: 10.5772/59467. Figure 3.

Research supported by a grant from the National Cancer Institute R25-CA134283 and the School of Medicine Summer Research Scholar Program.

The Anaphase Promoting Complex: A Novel Target In Cancer Therapy

Monzolesso J. Bagah-Kognagba[1], J. Mason Hoffman[1], B. Frazier Taylor[1], John O. Trent[2], J. Christopher States[1]
Departments of [1]Pharmacology & Toxicology and [2]Medicine
University of Louisville School of Medicine

Abstract

Background: The metaphase-anaphase transition is regulated by the spindle assembly checkpoint (SAC). The SAC ensures equal segregation of sister chromatids. The anaphase promoting complex/cyclosome (APC/C) is the master regulator of mitosis and is responsible for the metaphase-anaphase transition and licensing DNA replication in early G1. Without a functional APC/C, malignant cells arrest in mitosis or G1 state with subsequent cell death. Therefore, *in silico* studies were performed to predict hit compounds targeting the APC/C. **Hypothesis:** Hit compounds targeting the APC/C will induce mitotic arrest and apoptosis selectively in cancer cells. **Methods:** AlamarBlue, mitotic indices, and caspase-3/7 assays were performed with hit compounds in non-malignant HBEC3-KT cells and malignant A549 and H460 lung cells to determine the effect of these compounds on proliferation and induction of apoptosis. Photomicroscopy studies were performed prior to the caspase-3/7 assay to determine the optimal conditions for the assay. **Results:** AlamarBlue and mitotic index data show hit compounds reduce cell viability and increase mitotic index in all three cell lines. Photomicroscopy and caspase-3/7 assays show selective induction of apoptosis in malignant cells. **Discussion:** AlamarBlue assays do not differentiate between cytocidal and cytostatic activity. While hit compounds appear to reduce cell viability and increase mitotic index in both malignant and non-malignant cells, apoptosis assays indicate that only the malignant cells undergo apoptosis in response to mitotic arrest. This suggests that hit compounds are cytostatic, rather than cytotoxic in non-malignant cells.

Introduction

- Cancer is characterized by uncontrolled cell growth.
- Inhibition of cellular proliferation is a common chemotherapeutic strategy.
- Microtubule-targeting drugs such as paclitaxel inhibit cell cycle progression in mitosis.
- Paclitaxel is used in combination chemotherapy for multiple types of cancer, including lung cancer.
- Major issues with paclitaxel: Periodic shortage, neurotoxicity, and resistance[1].
- It is important to develop mitosis-inhibiting therapeutics with novel targets.
- A promising alternative strategy is targeting the anaphase promoting complex/cyclosome (APC/C), the master regulator of mitosis.
- The APC/C is a multisubunit E3 ubiquitin ligase necessary for mitotic and G1 progression.
- Inhibition of APC/C will result in cell cycle arrest in mitosis or G1, leading to apoptosis in cancer cells.

Hypothesis

- Hit compounds targeting the APC/C will induce mitotic arrest and apoptosis selectively in cancer cells.

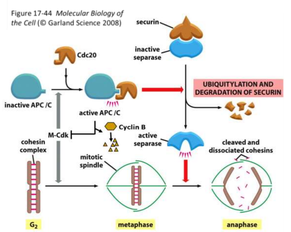

Figure 1. Role of APC/C as the master regulator of mitosis. APC/C targets cyclin B and securin for degradation to promote mitotic progression.

- Homology models of the catalytic subunits of the APC/C were generated and used for *in silico* screening to predict compounds to prevent their association.
- Inhibition of APC/C will result in cell cycle arrest in mitosis or G1, leading to apoptosis in cancer cells.

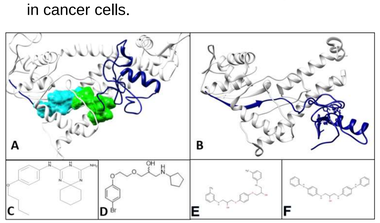

Figure 2. ANAPC2:ANAPC11 models and predicted inhibitor structures. (A) Homology structures of ANAPC11 (blue), ANAPC2-CTD (white) and sites targeted *in silico* (turquoise, green). (B) Published cryo-EM structure of ANAPC11 (blue) binding ANAPC2[2]. Structures of hit compounds 3 (C), 8 (D), 10 (E), and 11 (F). Note similarity of structures in A & B in the region of ANAPC11 binding.

Methods

AlamarBlue® Assays

- Immortalized human bronchial epithelial cells (HBEC3-KT) and adenocarcinoma (A549) and large cell carcinoma (H460) cell lines were plated in 96-well plates at 8000 cells/well for A549 and H460 cells and 2000 cells/well for HBEC3-KT cells.
- Cells were incubated for 24 h to allow proper attachment to the plate.
- Cells were treated with seven concentrations of hit compounds.
- AlamarBlue reagent (10% final volume) was added to each well at 44 h after treatment.
- Fluorescence was measured at 48 h at 590 nm (emission).

Mitotic Index Analysis

- HBEC3-KT, A549, and H460 cells were plated in triplicate at 150,000 cells/6 cm dish over three consecutive days and exposed to compounds.
- After 24 h, cells were harvested by trypsinization and swollen in 0.075 M KCl, fixed with methanol:acetic acid::3:1 (v/v) and dropped onto glass slides to burst the cell membrane. Cells were stained with Giemsa.
- Mitoses, catastrophes, and apoptoses were counted and are expressed as the percent of total nuclei counted (3 slides/sample, >200/ slide).

Phase Contrast Photomicroscopy

- HBEC3-KT, A549, and H460 cells were plated at 40,000 cells/well in a 24-well plate.
- Cells were incubated for 24 h to allow proper attachment to the plate.
- Cells were treated with five concentrations of hit compounds.
- Pictures were taken every 6 h for 48 h.
- Pictures were visually inspected to determine the timepoints of induction of apoptosis by each compound for each cell line.

Apo-One Caspase 3/7 Assay

- HBEC3-KT, A549, and H460 cells were plated at 7,500 cells/well in black-walled 24-well plates
- Cells were incubated for 24 h to allow proper attachment to the plate.
- Cells were treated with five concentrations of hit compounds.
- An equal volume of Apo-One caspase 3/7 reagent was added at 36 h.
- Plates were incubated at room temperature for 4 h following addition of the caspase 3/7 reagent.
- Fluorescence was measured at 499 (excitation) and 521 nm (emission).

Results (1)

Determination of Cellular Viability by AlamarBlue

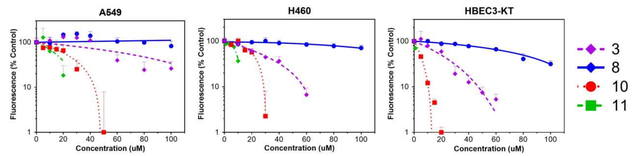

Figure 3. AlamarBlue assays show decreased viability in malignant A549 and H460 cells and nonmalignant HBEC3-KT cells. Paclitaxel (100 nM) and staurosporine (1 µM) were positive controls reducing cell viability to 8.8% and 0% respectively in HBEC3-KT cells and 0% in H460 and A549 cells for both controls. Fluorescence readings were normalized to values from DMSO-treated cells. Hit compounds show the same order of efficacy in decreasing viability in all three cell lines (11 > 10 > 3 > 8).

Mitotic Index Analysis

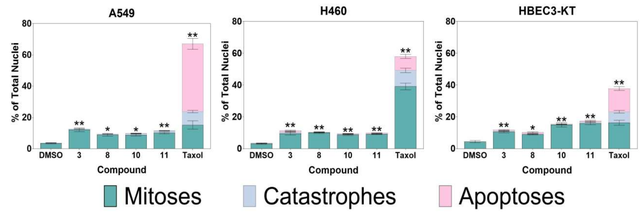

Figure 4. Hit compounds increase mitotic index in lung cell lines. Mitotic indices determined in A549, H460, and HBEC3-KT cells. Paclitaxel (100 nM) and compounds 3 (10 µM), 8 (60 µM), compound 10 (µM), and compound 11 (5 µM) were tested. Percent difference in mitoses was analyzed by one-way ANOVA (✱, P<0.05; ✱✱, P<0.01)

Results (2)

Caspase 3/7 Assay

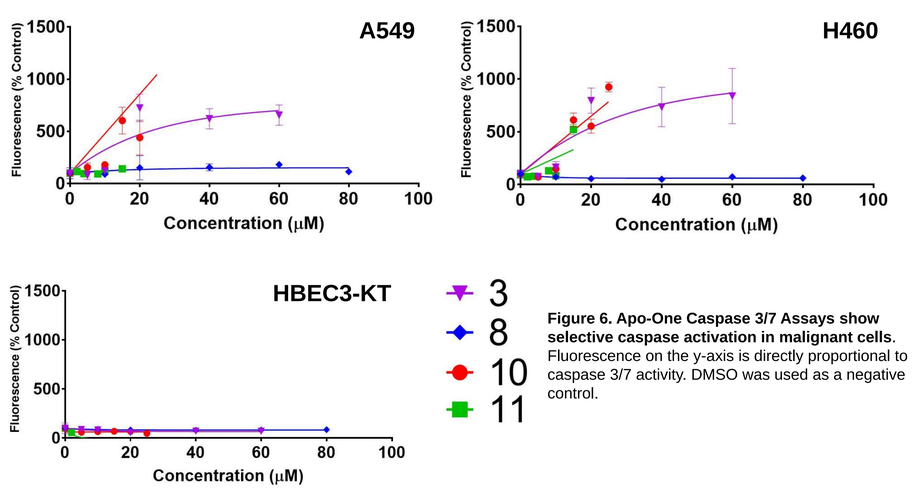

Figure 6. Apo-One Caspase 3/7 Assays show selective caspase activation in malignant cells. Fluorescence on the y-axis is directly proportional to caspase 3/7 activity. DMSO was used as a negative control.

Phase Contrast Photomicroscopy

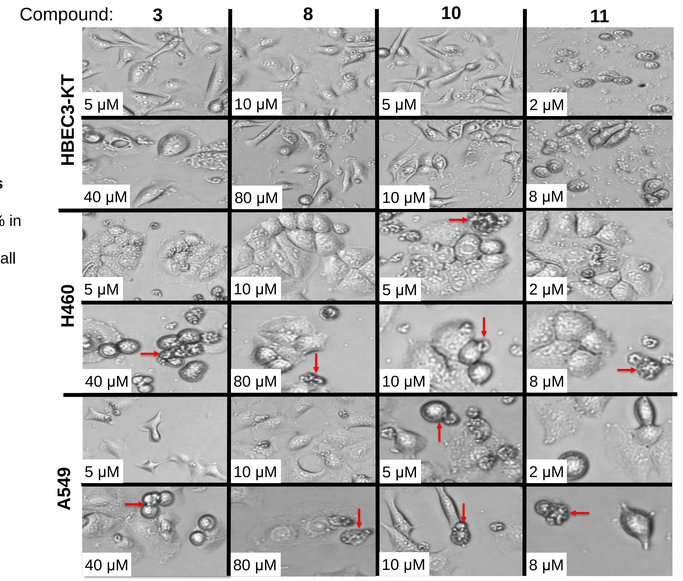

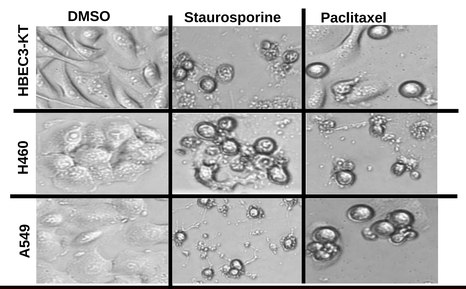

Figure 5: Induction of apoptosis detected by phase contrast photomicroscopy at 36 h. HBEC3-KT, H460, and A549 cells were plated and treated 24 h later with increasing concentrations of compounds 3 (0-60 µM), 8 (0-80 µM), 10 (5-25 µM), and 11 (0-15 µM) (Above). DMSO was used as a negative control. Paclitaxel (100 nM) and staurosporine (1 µM) were positive controls (Left). Apoptosis is characterized by membrane blebbing and indicated by the red arrows. For each compound, the highest concentration represents the maximum concentration tolerated by nonmalignant HBEC3-KT cells.

Conclusions

- Hit compounds arrested both malignant and nonmalignant cells in mitosis with selective induction of apoptosis in malignant cells, consistent with our hypothesis.
- These results suggest these compounds can undergo further structural modifications to candidate drugs that will induce cancer cell death while sparing normal cells.

References

1. Zhao, Y., Mu, X., & Du, G. (2016). Microtubule-stabilizing agents: New drug discovery and cancer therapy. *Pharmacology & Therapeutics,162*, 134-143.
2. Chang, L., Zhang, Z., Yang, J., Mclaughlin, S. H., & Barford, D. (2015). Atomic structure of the APC/C and its mechanism of protein ubiquitination. *Nature,522*(7557), 450-454.

Acknowledgements

Research supported by grants from National Cancer Institute (R25CA134283), Kentucky Lung Cancer Research Program (14-JCS-01), and Kentucky Science and Engineering Foundation (KSEF-3249-RDE-018).

Understanding Diagnostic Radiology Education During Undergraduate Medical Education

Ryan W. Bailer[1], Robert C. G. Martin II, MD, PhD[1]
University of Louisville School of Medicine, Department of Surgery, Division of Surgical Oncology[1]

Introduction

- Diagnostic radiology is an important competency that spans multiple medical specialties, and imaging is a necessary tool to evaluate patients in coordination with physical exam.
- However, it is often overlooked during medical education, so it is important to incorporate clinically relevant diagnostic radiology into clerkships during medical students' third and fourth years.
- The purpose of this study is to understand how diagnostic radiology is being taught, what barriers exist to increasing diagnostic radiology education, and possible solutions to those barriers.

Methods

Data for this project was collected from four sources:

1. A comprehensive review of the literature on diagnostic radiology education during undergraduate medical education, including curriculum, methods of teaching, and outcomes
2. AAMC Curriculum Inventory data on the subject of Radiology
3. A survey of clerkship directors at the University of Louisville in the departments of Emergency Medicine, Internal Medicine, Neurology, OB/GYN, and Surgery
4. The same survey sent to clerkship directors at other institutions

Results

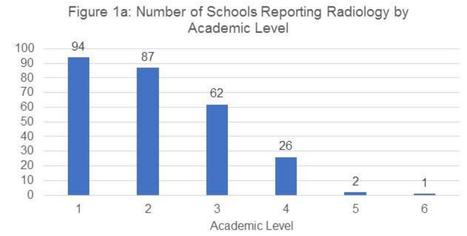

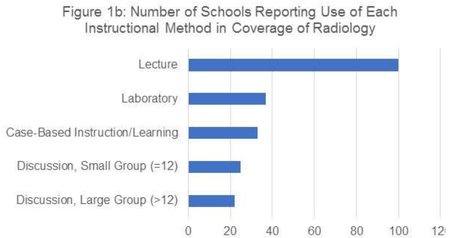

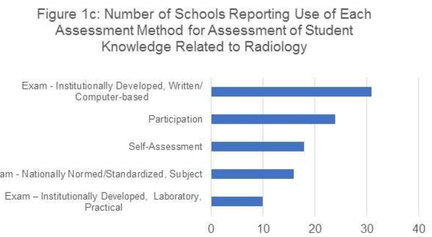

•**Fig. 1a:** Number of schools teaching radiology per academic year. Year 1 has highest number of schools reporting radiology education; the amount of radiology education decreases as the academic level increases.
•**Fig. 1b:** Number of schools reporting use of each instructional method to teach radiology.
•**Fig. 1c:** Number of schools reporting use of each assessment method to evaluate radiology knowledge.

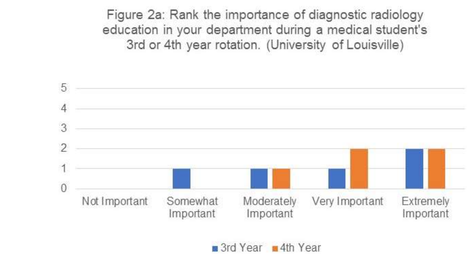

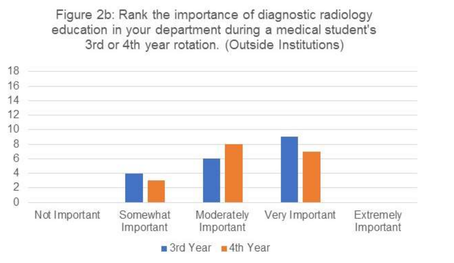

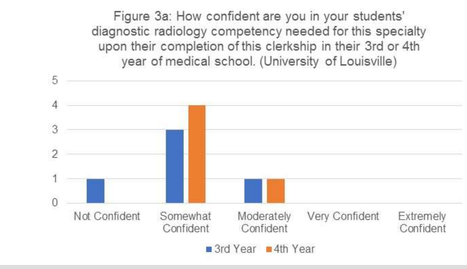

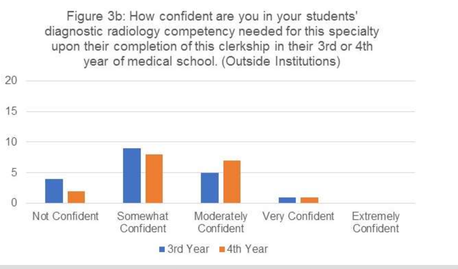

•**Fig. 2a:** Importance of diagnostic radiology in clerkships at the University of Louisville. 4/5 3rd year and 5/5 4th year clerkship directors indicate that radiology education is at least moderately important.
•**Fig. 2b:** Importance of diagnostic radiology in clerkships at other U.S. public medical institutions. 15/19 3rd year and 15/18 4th year clerkship directors indicate that radiology education is at least moderately important.
•**Fig. 3a:** Confidence in students' competency in radiology after completion of a clerkship at the University of Louisville. 4/5 3rd year and 4/5 4th year clerkship directors were either not confident or somewhat confident in students' diagnostic radiology competency upon completion of the clerkship.
•**Fig. 3b:** Confidence in students' competency in radiology after completion of a clerkship at other U.S. public medical institutions. 13/19 3rd year and 10/18 4th year clerkship directors were either not confident or somewhat confident in students' diagnostic radiology competency upon completion of the clerkship.

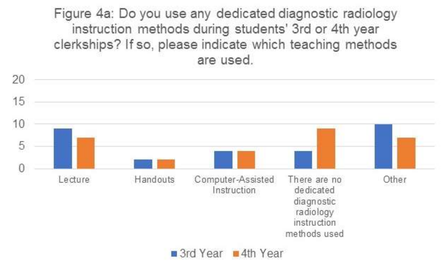

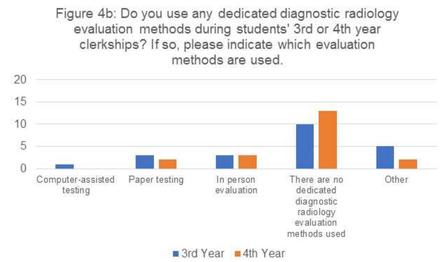

•**Fig. 4a:** Instruction methods used to teach diagnostic radiology during 3rd and 4th year clerkships at other U.S. public medical schools. Lecture is the most common method of instruction used. 4/19 3rd year and 9/18 4th year clerkship directors report no dedicated diagnostic radiology instruction. At the University of Louisville, 3/5 3rd year and 3/5 4th year clerkship directors report no dedicated diagnostic radiology instruction.
•**Fig. 4b:** Assessment methods used to evaluate diagnostic radiology competency at other U.S. public medical schools. 10/19 3rd year and 13/18 4th year clerkship directors report no dedicated diagnostic radiology evaluation methods used. At the University of Louisville, 5/5 3rd year and 5/5 4th year clerkship directors report no dedicated diagnostic radiology evaluation methods used.

Conclusions

- There is room for improvement for radiology education in U.S.
- Students, department heads, and medical school deans see value in radiology education
- Barriers exist to incorporating more radiology education, including time in the curriculum, faculty availability to teach, and financial constraints
- There are examples of initiatives to increase radiology education, including online modules, flipped classrooms, hands-on labs, simulation exercises, and externships and triage activities in a clinical setting with radiologists
- The future of successful radiology education will be vertical integration into preclinical medical education as well as integration into core clerkships that students are required to take

Acknowledgements

Research supported by a grant from the NCI R25 Grant, University of Louisville Cancer Education Program (R25-CA134283) and the School of Medicine Summer Research Scholar Program. I would also like to thank my mentor, Dr. Robert Martin II, MD, PhD for his guidance, and the AAMC for providing curriculum data on Radiology.

IDENTIFYING SERUM EXOSOMAL MICRORNA SIGNATURES AS DIAGNOSTIC TOOLS IN MELANOMA PATIENTS

Logan D. Carney[1], Kelly M. McMasters, M. D., Ph. D.[1] Hongying Hao, M.D., Ph.D.[1], Shesh N. Rai[2], Jianmin Pan[2],
Department of Surgery[1], University of Louisville School of Medicine
Biostatistics Shared Facility, Brown Cancer Center[2]

ABSTRACT

Introduction:
Early and accurate diagnosis of melanoma is challenging due to its heterogeneous nature and often unpredictable progression. Minimally invasive and reliable determinants that can sufficiently distinguish benign from malignant lesions and discern early from late stage disease status are needed. Exosomes are membranous, extracellular vesicles (~30-120 nm) that contain miRNA and are commonly secreted from tumor cells into the blood. Through miRNA array analysis, our previous research has revealed some differentially expressed exosomal miRNAs (exoRNAs) in stage I vs. non-melanoma subjects in a limited sample size. Further characterizing the differences in expression of exoRNAs between melanoma and non-melanoma as well as early stage and late stage melanoma patients could provide a novel method for an earlier, less invasive, and more dependable diagnostic measurement.
Hypothesis:
Identifying exoRNA signatures in melanoma patients of different disease stages will reveal molecular evidence of melanoma progression and provide a potential biomarker for enhanced melanoma diagnostics.
Methods:
In this study, exoRNAs were extracted from blood samples of stage I melanoma, stage IV melanoma, and non-melanoma (control) subjects using ExoRNeasy (dataset 1, n_1=24) and ExoQuick (dataset 2, n_2=24) isolation kits. Real-time RT-PCR was performed to confirm the differentially expressed exoRNAs in stage I vs. non-melanoma, stage IV vs. non-melanoma, stage IV vs. stage I, and all melanoma patients vs. non-melanoma controls in both datasets. The linear regression model was fit for ΔCt of each miRNA by group. The fold change and p-value of each miRNA was calculated with 95% confidence intervals.
Results:
A panel of differentially expressed exoRNAs was validated in stage I melanoma vs. non-melanoma controls. A specific group of exoRNAs was also found to be differentially expressed in stage IV vs. non-melanoma controls. Significant differences in the exoRNA profile of stage IV vs. stage I melanoma patients were also demonstrated. Some of these exoRNAs have been shown to actively participate in melanoma progression.
Conclusions:
The exoRNA signatures identified here may eventually lead to a minimally invasive yet reliable tool for the assessment of early diagnosis and disease progression in malignant melanoma.

INTRODUCTION

- Exosomes are 30-120 nm extracellular vesicles that contain mRNA, miRNA, and protein and are commonly found in body fluids.
- Exosomes are highly involved in cell-cell communication via autocrine and paracrine signaling.
- MicroRNAs (miRNAs) are small, single-stranded, noncoding RNA molecules that post-transcriptionally silence mRNA and regulate gene expression.
- Some of the miRNAs found in tumor exosomes have been shown to contribute significantly to the progression of malignant melanoma.
- Analyzing exosomal miRNA signatures in melanoma patients could identify a potential biomarker for early diagnostic assessment and prognosis.

METHODS

Patient Groups:
- Non-Melanoma
- Stage I Melanoma
- Stage IV Melanoma

1. Exosomes were isolated from patient serum using two separate isolation protocols - ExoRNeasy (Dataset 1) and ExoQuick (Dataset 2).
2. RNA was extracted from serum exosomes.
3. miRNAs were selected from previous experiments by Affymetrix miRNA array 2.0.
4. RT-PCR was performed to analyze and confirm differential expression of specific exosomal miRNAs among patient subsets in Dataset 1 and Dataset 2:
   - Stage I vs. Non-Melanoma
   - Stage IV vs. Non-Melanoma
   - Stage IV vs. Stage I Melanoma
   - Stage IV + Stage I vs. Non-Melanoma

DATASET 1 = ExoRNeasy
DATASET 2 = ExoQuick

METHODS

Non-Melanoma | Stage I Melanoma | Stage IV Melanoma

↓

Isolate serum exosome RNA using ExoRNeasy and ExoQuick isolation kits

↓

Confirm differential expression with RT-PCR analysis

↓

Analysis and Comparison of Dataset 1 and Dataset 2:
Stage I vs. Non-Melanoma | Stage IV vs. Stage I Melanoma
Stage IV vs. Non-Melanoma | Stage IV + Stage I vs. Non-Melanoma

Figure 1. Assay Workflow

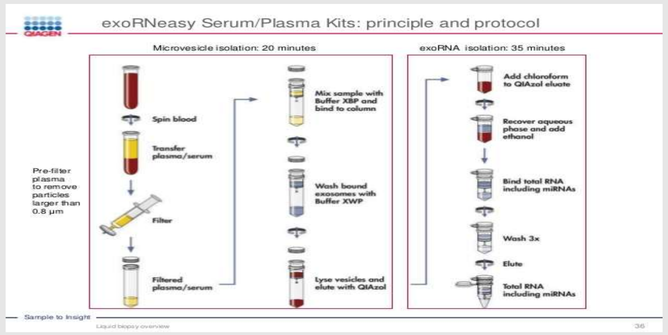

Figure 2. ExoRNeasy Isolation Kit Protocol – DATASET 1

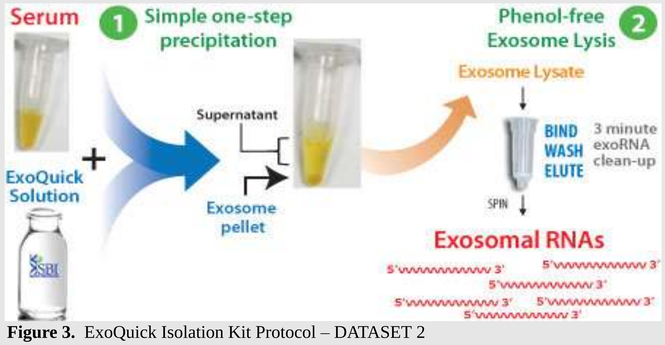

Figure 3. ExoQuick Isolation Kit Protocol – DATASET 2

RESULTS

PATIENT GROUP	TOTAL N		SEX (M/F)		AGE RANGE		MEAN AGE	
	DATASET 1	DATASET 2	DATASET 1	DATASET 2	DATASET 1	DATASET 2	DATASET 1	DATASET 2
Non-Melanoma	8	8	4/4	4/4	46-68	32-79	58.8	53
Stage I Melanoma	8	8	4/4	4/4	31-67	23-88	55.9	65.1
Stage IV Melanoma	8	8	4/4	4/4	36-72	27-81	50.4	61.5

Table 1. Patient Demographics

Table 2. Fold changes of differentially expressed miRNAs in Stage I vs. non-melanoma patients

	DATASET 1 (n=16)		DATASET 2 (n =16)	
miRNAs	Fold Change	P-Value	Fold Change	P-Value
miR-1	3.85	0.480	6.32	0.317
miR-2	15.21	0.210	7.19	0.206
miR-5	4.18	0.496	1.64	0.722
miR-10	0.18	0.209	4.07	0.307
miR-11	0.47	0.437	8.68	0.156
miR-9	0.11	0.039	3.89	0.484
miR-3	0.50	0.518	16.84	0.208
miR-4	0.79	0.781	6.95	0.048
miR-12	0.34	0.318	10.89	0.066
miR-7	1.30	0.831	8.04	0.127
miR-13	0.06	0.028	26.92	0.082

Table 3. Fold changes of differentially expressed miRNAs in Stage IV vs. non-melanoma patients

	DATASET 1 (n=16)		DATASET 2 (n=16)	
miRNAs	Fold Change	P-Value	Fold Change	P-Value
miR-2	27.35	0.232	0.52	0.688
miR-12	0.12	0.080	1.12	0.929
miR-3	0.24	0.164	6.82	0.448
miR-4	0.71	0.696	3.26	0.362
miR-13	1.50	0.734	79.12	0.037

Table 4. Fold changes of differentially expressed miRNAs in Stage IV vs. Stage I melanoma patients

	DATASET 1 (n=16)		DATASET 2 (n=16)	
miRNA s	Fold Change	P-Value	Fold Change	P-Value
miR-5	0.11	0.030	0.08	0.115
miR-10	1.13	0.916	0.08	0.053
miR-11	0.59	0.640	0.04	0.032
miR-2	1.80	0.544	0.08	0.024
miR-12	0.36	0.335	0.10	0.039
miR-7	0.43	0.315	0.13	0.063
miR-13	26.80	0.005	2.94	0.484

Table 4. Fold changes of differentially expressed miRNAs in Stage IV + Stage I vs. non-melanoma patients

	DATASET 1 (n=24)		DATASET 2 (n=24)	
miRNA s	Fold Change	P-Value	Fold Change	P-Value
miR-1	2.32	0.531	3.12	0.491
miR-2	19.43	0.087	2.45	0.481
miR-3	0.34	0.183	11.99	0.173
miR-9	0.17	0.052	1.77	0.759
miR-6	0.19	0.095	0.01	0.121
miR-4	0.75	0.647	4.90	0.122
miR-12	0.21	0.106	3.49	0.239
miR-7	0.85	0.872	2.94	0.308
miR-13	0.29	0.330	46.15	0.019

- Exosomal miRNAs miR-4 miR-12, and miR-13 reflected significant fold changes in Stage I melanoma patients vs. non-melanoma controls.
- Exosomal miRNA miR-13 displayed significant fold changes in Stage IV vs. non-melanoma controls.
- Exosomal miRNA miR-13 demonstrated significant changes in Stage IV vs. Stage I melanoma subjects.
- Exosomal miRNAs miR-2 and miR-13 exhibited significant changes in melanoma vs. non-melanoma patients (non-specific to disease stage).
- Exosomal miR-13 is of particular interest, as it was shown to be consistently upregulated as melanoma disease stage progressed.

CONCLUSIONS

- Specific exosomal miRNAs were found to be differentially expressed as a function of melanoma disease status - many of which were consistently downregulated.
- These differences in miRNA expression allow for alterations in gene regulation that are thought to play a crucial role in the development and progression of malignant melanoma.
- Our results provide evidence that further characterization of exosomal miRNA signatures in melanoma patients of varying disease stages is warranted.
- This research could eventually lead to the development of a minimally invasive method for specific and early diagnosis of malignant melanoma.

ACKNOWLEDGEMENTS

Research supported by NCI R25 grant University of Louisville Cancer Education Program NIH/NCI (R25-CA134283), grant from Melanoma Research Foundation, and University of Louisville Clinical & Translational Science Pilot Grant Innovative Award to K.M.M.

UNIVERSITY OF LOUISVILLE
It's Happening Here.®

UBQLN1 Regulates Expression of EGFR^{WT} but not EGFR^{mut} in Lung Adenocarcinoma Cells

Rain Dunaway[1], Zimple Kurlawala[2], Parag Shah[3], and Levi J. Beverly[1,3]

School of Medicine[1], Department of Neurology[2], Department of Pharmacology/Toxicology[3], University of Louisville, Louisville, KY

Role of EGFR in Tumorigenesis

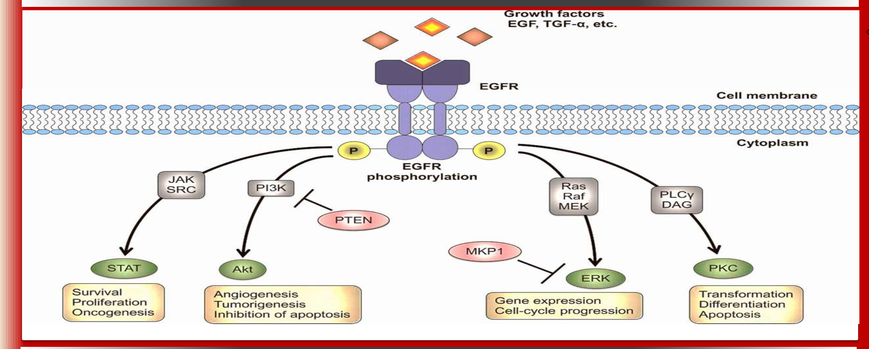

Abstract

Introduction: Lung cancer is the second most common cancer in men and women and the leading cause of cancer-related deaths worldwide. Adenocarcinomas represent approximately 40% of all lung cancer cases. Epidermal Growth Factor Receptor (EGFR) is a tyrosine kinase receptor involved in proliferation pathways. Mutations in the EGFR gene, a known oncogene, account for 10-15% of adenocarcinoma cases. Of the known mutations, some make adenocarcinomas more sensitive to treatment with tyrosine kinase inhibitors (TKIs), while other mutations increase resistance to TKIs. The Ubiquilin family is a family of proteins that have ubiquitin-like functions and are also involved in regulation of proteins like anti-apoptotic BCLb and another receptor tyrosine kinase, IGF1R. UBQLN1 function is lost in 50% of lung adenocarcinoma cases. The Beverly lab has discovered an interaction between EGFR and UBQLN1. We aim to study regulation of EGFR by UBQLN1 and implications of this association in lung cancer progression.

Objective: We hypothesize that UBQLN1 regulates EGFR expression and activity, and that loss of UBQLN1 makes lung adenocarcinoma cells more tumorigenic.

Methods: We used two lung adenocarcinoma cell lines in our studies: A549 (EGFR^{WT}, K-RAS^{G12S}) and H1650 (EGFR^{A746del750}, K-RAS^{WT}). We studied regulation of EGFR by UBQLN1 using the following methods: Immunoprecipitation, Western Blot analysis, Alamar Blue assay, and qRT-PCR.

Results: We found that following loss of UBQLN1 in A549 cells, there is decreased expression of EGF receptors when stimulated with EGF compared to wild-type. However, the ratio of phosphorylated to total EGFR is higher in cells with loss of UBQLN1 function. In H1650 cells, we did not find such a difference.

Conclusion: We conclude that UBQLN1 is critical in regulation of wild-type EGFR but not constitutively active EGFR. Loss of UBQLN1 leads to persistent stimulation of EGFR which may contribute to tumorigenic events in UBQLN1 deficient cells that have wild-type EGFR. Therefore, this receptor could be an appropriate target in EGFR^{WT} cancers that have loss of UBQLN1 function.

Hypothesis

We hypothesize that UBQLN1 regulates EGFR expression and activity, and that loss of UBQLN1 makes lung adenocarcinoma cells more tumorigenic.

UBQLN Structure

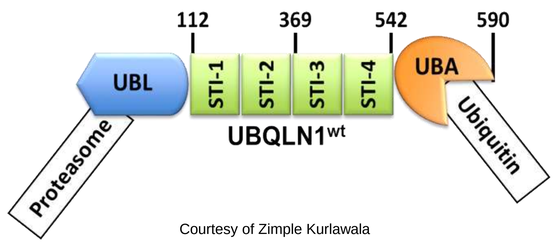

Courtesy of Zimple Kurlawala

Results

1 EGFR Interaction

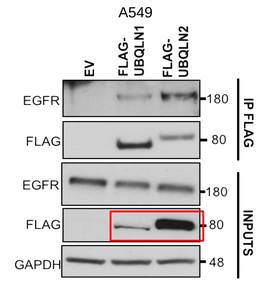

Courtesy of Parag Shah

2 Dose Response

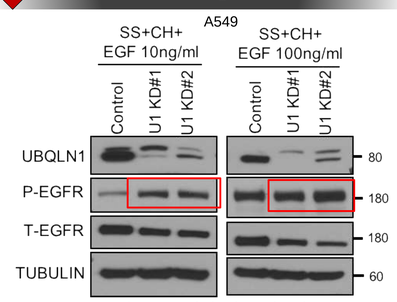

Courtesy of Zimple Kurlawala

3 mRNA Transcription

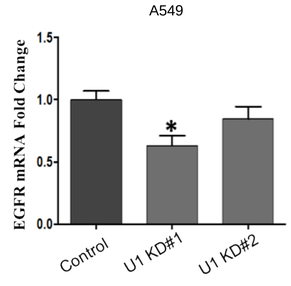

Courtesy of Zimple Kurlawala

5 Degradation Kinetics

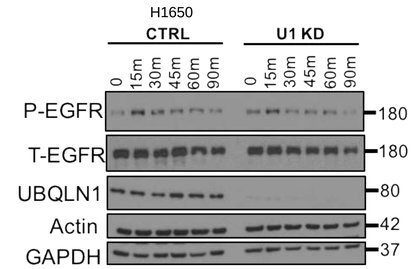

4 Steady State Expression

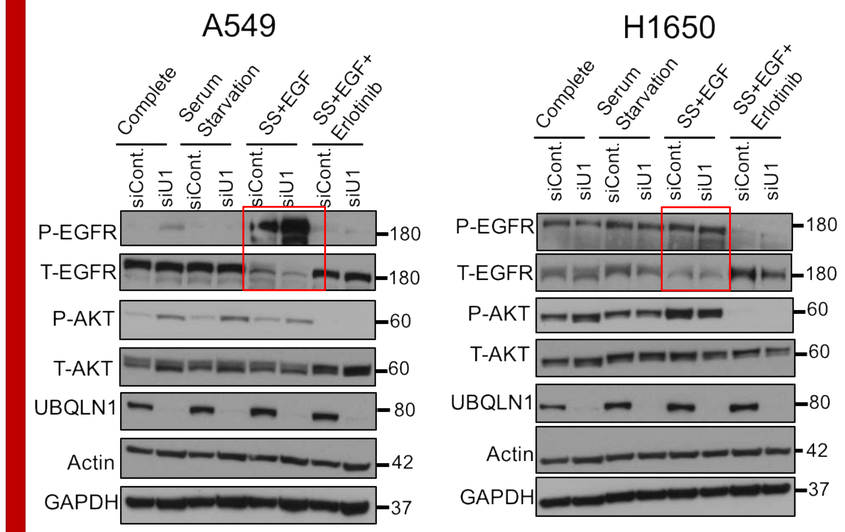

6 Degradation Kinetics

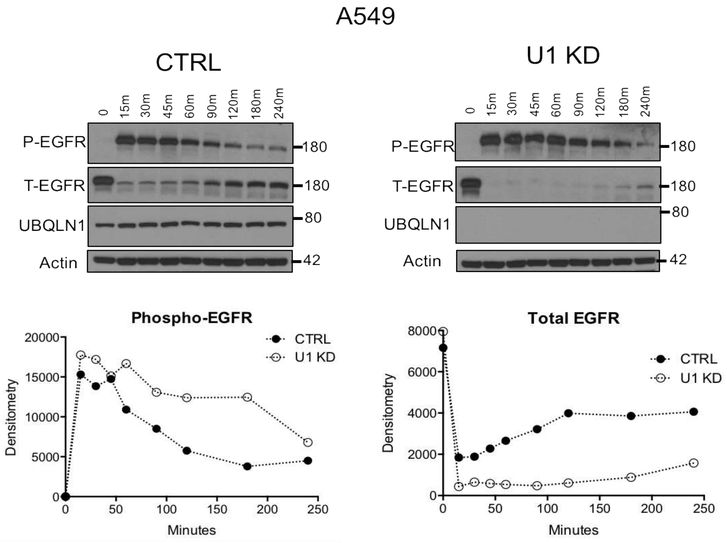

Conclusions

- Expression of phosphorylated EGF receptors increases in UBQLN knockdown vs control in A549 cells
- Expression of total EGF receptors decreases in UBQLN knockdown vs control in A549 cells
- Ratio of P-EGFR:T-EGFR is higher in U1 KD A549 cells
- Do not see similar patterns in H1650 cells
- Caveat: data is still in preliminary stages

Future Directions

- Look at number of EGF receptors in the presence of Bortezomib, a proteasomal inhibitor
- Repeat degradation kinetics experiment in the presence of Cyclohexamide, an inhibitor of de novo protein synthesis
- Check for receptor saturation at higher dose of EGF

Acknowledgements

Research was supported by the NCI R25-CA134283 Cancer Education Program grant, the NCI R01-CA193220 grant, and the James Graham Brown Cancer Center.

IDENTIFICATION OF THE ENDOGENOUS ROLE OF ARYLAMINE N-ACETYLTRANSFERASE 1 IN CANCER RELATED CELLULAR PROCESSES THROUGH PROTEOMIC ANALYSIS

Jonathan Q. Gardner[1,2], Marcus W. Stepp[1,2], Daniel W. Wilkey[1,3], Michael L. Merchant[1,3], David W. Hein[1,2]

[1]University of Louisville School of Medicine, [2]Department of Pharmacology and Toxicology,
[3]Department of Medicine, Division of Nephrology and Hypertension

ABSTRACT

Background- Arylamine N-acetyltransferase 1 (NAT1) is a cytosolic enzyme that catalyzes the transfer of acetyl groups onto various substrates which usually include but are not limited to aromatic amines and hydrazines. Currently, xenobiotic metabolism is the most predominant and well known role of NAT1 but the potential endogenous role of this enzyme has been a focus of recent study. There is evidence showing variable NAT1 expression is associated with varying intracellular amounts of acetyl CoA, cell-cell contact propensity, and presence of malignant breast cancer tumors in rats. The mechanisms are currently unknown. In order to better understand NAT1's role in cancer its endogenous role must be further explored.
Hypothesis- In this study, we compare NAT1 CRISPR knockout cells to the parental MDA-MB-231 triple negative breast cancer cell line in proteomic analysis to explore possible pathways that are affected by varying NAT1 expression between the cell lines. We hypothesized that a comparative proteomics analysis of parental versus NAT1-KO cell lines would identify differences in proteins important for the observed phenotypic differences of cellular adhesion, intracellular acetyl CoA levels, and tumorigenic pathways.
Methods- Two unique guide RNAs were utilized in CRISPR/Cas9 to knockout NAT1 activity to generate two unique MDA-MB-231 cell lines. Two knockout cell lines were compared to parental. Quantitative proteomic analysis was used to analyze global protein levels which was further analyzed using Metacore software to rank cellular pathways most likely affected by absence of NAT1 activity.
Results- Proteomic data comparing parental and knockout cell lines showed differing relative protein abundance in many cellular pathways including cell adhesion, immune response, and cytoskeleton remodeling.
Conclusion- This data further supports the indication of an endogenous role for NAT1 especially in cell adhesion processes. Verifying these results through additional assays for specific proteins of interest would strengthen these findings. These results can then be used to guide further understanding of NAT1 and its endogenous role.

HYPOTHESIS

We hypothesized that a comparative proteomics analysis of parental versus NAT1-KO cell lines would identify differences in proteins important for the observed phenotypic differences of cellular adhesion, intracellular acetyl CoA levels, and tumorigenic pathways.

METHODS

Cell lines- Two guide RNAs were implemented in the CRISPR Cas9 system to generate two unique Arylamine N-Acetyltransferase 1 knockouts (#2 and #5) in MDA-MB-231 triple negative breast cancer cells. Protein lysates were compared from these two NAT1 knockout cell lines and the parental cell line.
Proteomics- Quantitative Proteomics involving Liquid Chromatography–Mass Spectroscopy/Mass spectroscopy (LC-MS/MS) was used to acquire global protein levels in 3 samples of each cell lysate from Parental, #2, and #5 cell lines. Scaffold software was used with the following parameters: protein threshold of 99.9%, minimum number of peptide = 1, and peptide threshold of 99.9%. Protein species were normalized to the average of the 9 samples. This yielded 4890 proteins with a false discovery rate of 0.389%. Protein species concentration in knockouts were transformed to log2 fold change relative to parental concentrations. Metacore software was used to analyze protein fold changes between cell lines and predict probable cellular pathways affected by NAT1 knockout. Prism software was use to conduct one-way ANOVA and a Bonferroni multiple comparison post-test to calculate statistical significance between select proteins in parental verses #2 or #5 knockouts. The following symbols are used to indicate respective level of p-value significance: * < 0.05, ** < 0.01, and *** < 0.001.

RESULTS

Table 1 – Top 15 Pathways

Rank	Pathway	P-Values[1]	Ratio[2]
1	Immune response- Antigen presentation by MHC class I, classical pathway	4.552e-21 4.873e-21	41/54 41/54
2	Cytoskeleton remodeling- Cytoskeleton remodeling	6.917e-18 1.940e-19	56/102 58/102
3	Transport- Clathrin-coated vesicle cycle	3.601e-16 3.848e-16	43/71 43/71
4	LRRK2 in neurons in Parkinson's disease	2.735e-13 1.801e-14	25/33 26/33
5	Cytoskeleton remodeling- TGF, WNT and cytoskeletal remodeling	2.184e-12 2.716e-14	51/111 54/111
6	Apoptosis and survival- NGF/ TrkA PI3K-mediated signaling	7.391e-13 1.373e-13	41/77 42/77
7	Development- Regulation of cytoskeleton proteins in oligodendrocyte differentiation and myelination	2.428e-13 2.562e-13	35/58 35/58
8	Oxidative phosphorylation	2.563e-13 2.749e-13	50/103 50/103
9	Apoptosis and survival- Granzyme B signaling	2.735e-13 2.851e-13	25/33 25/33
10	Cell cycle- Spindle assembly and chromosome separation	2.735e-13 2.851e-13	25/33 25/33
11	Transcription- Negative regulation of HIF1A function	1.207e-12 1.275e-12	37/66 37/66
12	Cell adhesion- Chemokines and adhesion	2.503e-11 6.233e-12	46/100 47/100
13	Regulation of degradation of deltaF508-CFTR in CF	1.011e-10 1.161e-11	25/39 26/39
14	Cell cycle Chromosome condensation in prometaphase	1.472e-11 1.518e-11	18/21 18/21
15	Cell adhesion Role of tetraspanins in the integrin-mediated cell adhesion	1.779e-11 1.851e-11	25/37 25/37

[1]Statistical significance of a difference in cellular pathway enzymes between knockout cell line and parental.
[2]Number of enzymes quantitatively identified in proteomic analysis over total number of enzymes in Metacore pathway.

UofL Design and Print

RESULTS

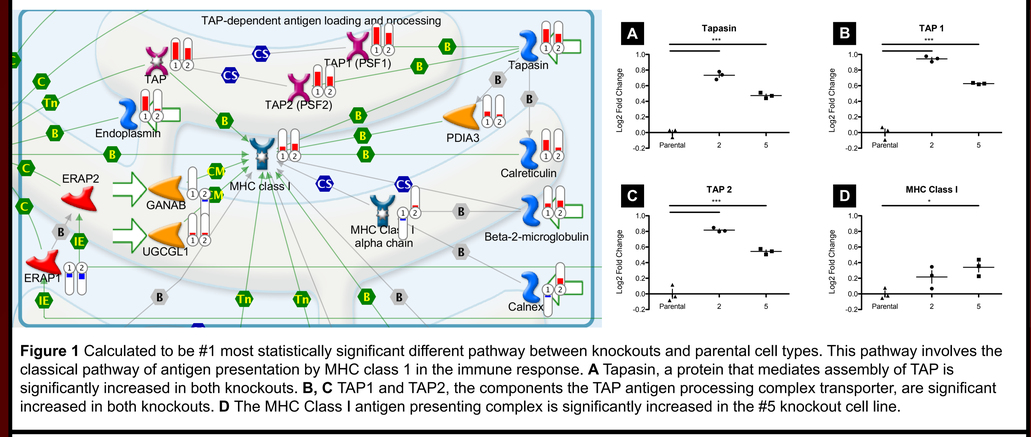

Figure 1 Calculated to be #1 most statistically significant different pathway between knockouts and parental cell types. This pathway involves the classical pathway of antigen presentation by MHC class 1 in the immune response. **A** Tapasin, a protein that mediates assembly of TAP is significantly increased in both knockouts. **B, C** TAP1 and TAP2, the components the TAP antigen processing complex transporter, are significant increased in both knockouts. **D** The MHC Class I antigen presenting complex is significantly increased in the #5 knockout cell line.

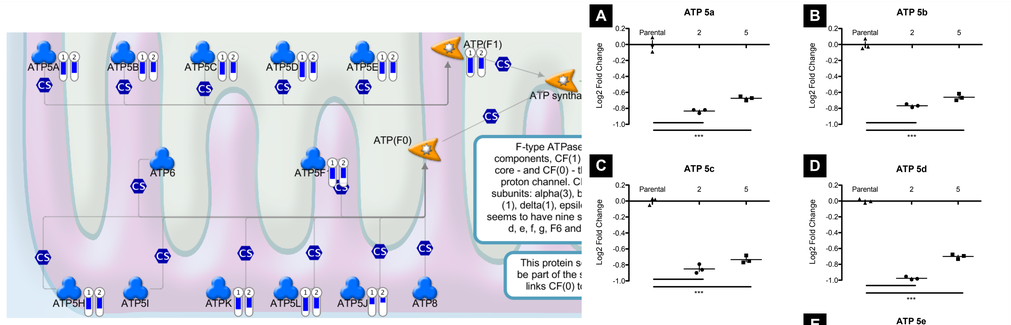

Figure 2 Calculated to be #8 most statistically significant different pathway between knockouts and parental cell types. This pathway involves mitochondrial oxidative phosphorylation, specifically ATP synthase, a protein that utilizes the electrochemical gradient across the inner mitochondrial membrane to synthesize high energy ATP molecules. All 5 subunits of ATP synthase, alpha (**A**), beta **(B)**, gamma **(C)**, delta **(D)**, and epsilon **(E)** were significantly decreased in both knockout cell lines.

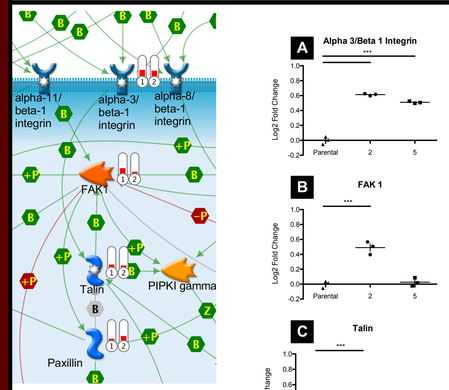

Figure 3 Calculated to be #12 most statistically significant different pathway between knockouts and parental cell types. This pathway involves chemokine signaling and cell adhesion. **A** Alpha-3/beta-1 integrin, used to recruit adhesion proteins when activated, is significantly increased in both knockouts. **B** Focal Adhesion Kinase 1, a protein that stimulates cytoskeleton remodeling through phosphorylation, is significantly increased in the #2 knockout. **C** Talin, used to link integrin clusters to the cytoskeleton, is significantly increased in the #2 knockout. **D.** Paxillin, having a similar role as Talin, is significantly increased in the #5 knockout.

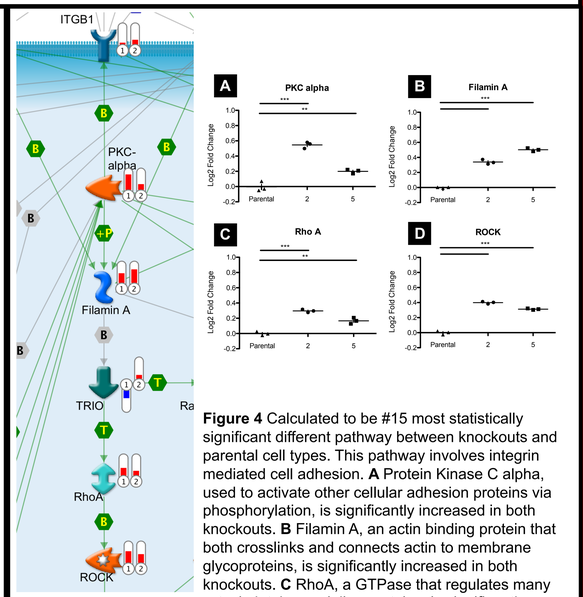

Figure 4 Calculated to be #15 most statistically significant different pathway between knockouts and parental cell types. This pathway involves integrin mediated cell adhesion. **A** Protein Kinase C alpha, used to activate other cellular adhesion proteins via phosphorylation, is significantly increased in both knockouts. **B** Filamin A, an actin binding protein that both crosslinks and connects actin to membrane glycoproteins, is significantly increased in both knockouts. **C** RhoA, a GTPase that regulates many cytoskeletal remodeling proteins, is significantly increased in both knockouts. **D.** ROCK, a serine/threonine kinase involved in focal adhesion regulation among other pathways, is significantly increased in both knockouts.

RESULTS

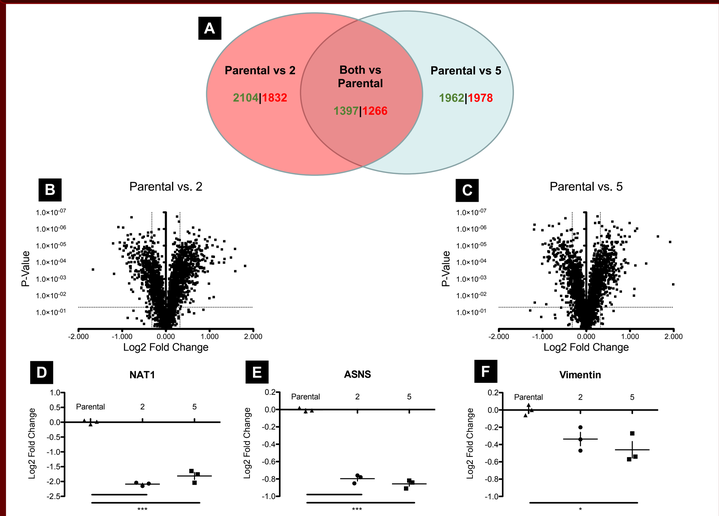

Figure 5 A Venn diagram showing total protein species concentrations increased (green) and decreased (red) in parental verses #2 knockout, parental verses #5 knockout, and parental verses #2 and #5 knockouts. Volcano plot showing fold change verses p-value of difference in protein species concentration between #2 knockouts **(B)** and #5 knockouts **(C)**. **D** Arylamine N-acetyltransferase 1 is shown to be dramatically decreased in both knockouts verifying CRISPR as an effective means to knock out the targeted protein. **E** Asparagine synthase, an essential enzyme involved in cell proliferation, is shown to be significantly decreased in both knockouts. **F** Vimentin, an intermediate filament protein involved in cellular stress resistance, is shown to be decreased in both knockouts.

DISCUSSION

Pathway analysis generated through Metacore software yielded interesting potential pathways effected by endogenous NAT1 activity. Among the top 15 pathways generated, antigen presentation by MHC class I, oxidative phosphorylation, and 2 cellular adhesion pathways were more closely studied due to the presence of 3 or more consecutive proteins in a pathway showing similar changes in protein amount between knockouts. Many proteins in Tapasin-dependent antigen presentation were significantly increased in knockouts **(Figure 1)**. This MHC class 1 antigen presentation process is integral in the cancer immune response through signaling cytotoxic T Cell mediated apoptosis. In fact, a well-known mechanism of many cancers is the downregulation of MHC molecules. Increased expression of MHC 1 suggests possibly a more effective immune response in knockouts compared to parental. ATP synthase expression has also been found to differ in many cancers. As the rate of cellular proliferation is higher in many cancers relative to normal tissue, the cellular energy requirement for cancer cells is increased and ATP synthase expression is upregulated. Both knockouts were shown to have decreased amounts of every measured subunit of ATP synthase while other mitochondrial proteins in this pathway did not follow a similar trend **(Figure 2)**.This may indicate a less aggressive cancer phenotype in knockouts. Previous studies involving NAT1 knockouts had suggested a potential role in cellular adhesion pathways. In these studies, knockouts were shown to have decreased anchorage independent colony formation (soft agar assays). Additional experimentation observed increased cellular adhesion in NAT1 knockouts via suspended drop assay. Interestingly, Metacore analysis showed a high probability of many cellular adhesion pathways being affected in NAT1 knockout cell lines. Among these are pathways including Focal Adhesion Kinase 1 (FAK1), a protein that's expression plays an important role in cellular migration and attachment **(Figure 3)**. Increased expression of FAK1 has been shown to increase the metastatic potential of cancer cells leading to a poorer prognosis. Pathways including Protein Kinase C alpha (PKC alpha) are also shown to be effected in knockouts **(Figure 4)**. This protein is known to have a wide variety of cellular functions involving cell adhesion, transformation, and cell cycle checkpoints and is a popular area of research because of its known involvement in oncogenic processes. Although statistically limited by a lack of measured proteins in their pathway, some proteins showed significant differences between parental and knockout lines. Among these are Asparagine Synthase (ASNS) and Vimentin **(Figure 5)**. ASNS, an enzyme utilized in asparagine synthesis, was shown to be significantly decreased in both knockouts. Cellular asparagine is needed for extracellular amino acid exchange, especially serine, threonine, and arginine. Unavailability of serine specifically has negative effects on nucleotide synthesis which is needed in cellular proliferation. Vimentin, an intermediate filament protein involved in cellular stress resistance, was shown to be decreased in both knockouts. Vimentin plays a role in cellular organization and has been shown to be upregulated in many cancers. Recent evidence has shown Vimentin's role in epithelial to mesenchymal transition (EMT), a known step in metastatic cancer progression. These findings provide insight into the mechanisms behind previous laboratory findings regarding NAT1 including its role in cellular adhesion and tumorigenic processes.

FUTURE DIRECTION

These findings provide the groundwork for a mechanistic approach to NAT1 endogenous activity and can be used to guide a targeted approach to certain cellular pathways in the future. Verification of the effected protein species indicated in this study is required through protein immunoblots or mRNA PCR.

ACKNOWLEDGEMENTS

Research funded at the University of Louisville by the National Cancer Institute R25 CA-134283 Cancer Education Program Grant and Liver Hepatobiology and Toxicology COBRE grant P20GM113226 (CJ McClain, MD, PI) (MLM, DWH). I would also like to acknowledge the efforts of Mark Doll for helping in the construction of NAT1 knockout cell lines.